2013 IEEE/RSJ International Conference on
Intelligent Robots and Systems (IROS)
November 3-7, 2013. Tokyo, Japan

Maximal Output Admissible Set for Trajectory Tracking Control of Biped Robots and its Application to Falling Avoidance Control

Ko Yamamoto

Abstract— **Humanoid robots have been considered as a universal machine which can operate in place of human. This kind of universal machine requires human-like biped walking capability. In particular, it is important to avoid falling by appropriately switching behaviors even if there are unknown disturbances. The authors proposed the maximal output admissible (MOA) set for the center of gravity (COG) regulator in the upright position. Based on the MOA set, we can switch feedback gains with the Zero Moment Point (ZMP) constraint satisfied. In this paper, the author extends MOA set framework to trajectory tracking controller. This extension makes it possible to switch controllers: regulator in the upright position and tracking controller of a stepping motion in order to avoid falling. The effectiveness of the proposed method is verified with a simulation.**

I. Introduction

Humanoid robots have been considered as a universal machine which can operate in place of human. This kind of universal machine requires human-like biped walking capability. In particular, it is important to avoid falling by appropriately switching its behaviors even if there are unknown disturbances. However, motion control of biped humanoid robots is a challenging problem because the biped robot is a floating-base system and there exists a constraint on contact force between the robot and environment, which is also called *physical constraint*. There have been a lot of research on biped walking control. Those research can be divided into A) tracking control with time-variant referential trajectory, and B) autonomous control without referential trajectory. Concerning A), a lot of researchers proposed biped gait planning methods [1], [2], [3], [4], [5]. In those research, a biped gait is planned so that the physical constraint is satisfied. While the planned gait is used as a reference, a robot is controlled with compensation of modeling errors, for example, modulation of foot landing position, leg impedance control for uneven terrain, or body attitude compensation. These controllers make a robot track the referential trajectory as precisely as possible. Therefore, it is difficult to absorb large disturbances by changing robot behaviors. Although motion database [6] was proposed to generate various motions, connecting different motions requires dynamics filtering [7].

Concerning B), on the other hand, there are studies on B1) balancing in the upright position [8], [9], [10], [11], B2) limit cycle type control [12], [13], [14], [15] and B3) optimal control scheme [16] or model predictive control [17]. In B1), Abdallah et al.[10] and Atkeson et al.[11] proposed a control method to switch the hip joint and ankle joint control. In B2), Stephens et al. [14] and Sugihara [15] proposed a control method to switch a balancing controller in the upright position and a limit cycle type controller for periodic stepping. They defined *stabilizable region* in the state space for each controller, and switched controllers based on that. The authors [18] applied the Maximal Output Admissible (MOA) set framework to a regulator of the center of gravity (COG) in the upright position. The MOA set [19][20] was proposed in the control engineering field. Using the MOA set, we can determine if the constraint on the Zero Moment Point (ZMP) [21] will be satisfied or not when a regulator is applied for the COG stabilization. We can also switch feedback gains for the regulator based on the MOA set. In [18], the MOA set was defined for a constant support polygon. If we extend the MOA set framework to A) trajectory tracking controller, B2) limit cycle type controller or B3) optimal control and model predictive control, we can switch various motion controllers with the physical constraint satisfied.

In this paper, we present the MOA set for trajectory tracking control with as one of extensions of the MOA set framework. Although Kogiso et al. [22] proposed the MOA set for time-variant reference by parallel shifting the MOA set for a regulator, they assumed a constant constraint. In the biped system, we need to consider time-variant constraint as the support polygon changes. In Sect. II, the author formulates a state equation and the ZMP constraint for the inverted pendulum model of a biped robot. Then, the MOA set on the COG regulator is presented in Sect. III. In Sect. IV, the author proposes computational procedure of the MOA set for trajectory tracking control, and present an example of computation for a biped walking motion. Moreover, the MOA set framework is applied to falling avoidance control in Sect. V. It is verified with a simulation that we can switch the COG regulator and trajectory tracking controller depending on disturbances. In Sect. VI, the author summarizes this paper and addresses future works.

II. COG-ZMP Inverted Pendulum Model

Suppose that a biped robot moves on a flat ground as shown in Fig. 1(a). Then, let x- and z- axes be moving direction and vertical direction, respectively. We can set the origin of z-axis on the ground without loss of generality. Let $\boldsymbol{p}_G = [\ x_G\ y_G\ z_G\ ]^T$ and $\boldsymbol{p}_Z = [\ x_Z\ y_Z\ 0\ ]^T$ denote the COG and ZMP, respectively. Assuming the total mass

This research is supported by Grant-in-Aid for Young Scientists (B) #25820086, Japan Society for the Promotion of Science.

The authors is with the EcoTopia Science Institute, Nagoya Univ., Furo-Cho, Chikusa-Ku, Nagoya 464-8603, Japan. ko.yamamoto@esi.nagoya-u.ac.jp

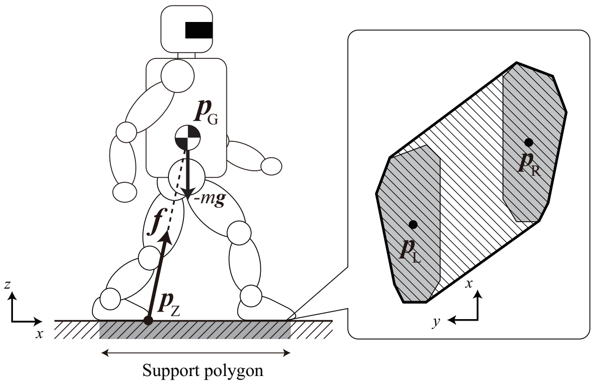

Fig. 1. COG-ZMP inverted pendulum model

is concentrated at the COG, horizontal motion equations are formulated as follows:

$$\ddot{x}_G = \omega^2(x_G - x_Z) \tag{1}$$
$$\ddot{y}_G = \omega^2(y_G - y_Z) \tag{2}$$
$$\omega^2 := \frac{\ddot{z}_G + g}{z_G}. \tag{3}$$

where g is the gravity acceleration. In this paper, we focus on biped walking with constant COG height, namely, $z_G =$ const. and $\ddot{z}_G = 0$. Therefore, we can assume ω^2 is also constant. Equations (1) and (2) are equivalent to inverted pendulum dynamics as shown in Fig. 1(b). We call this model *COG-ZMP inverted pendulum model*.

Now, we choose the COG and its velocity as the state variable $\boldsymbol{x}$ and the ZMP as the control input $\boldsymbol{u}$.

$$\boldsymbol{x} = \left[\begin{array}{cccc} x_G & \dot{x}_G & y_G & \dot{y}_G \end{array}\right]^T \tag{4}$$
$$\boldsymbol{u} = \left[\begin{array}{cc} x_Z & y_Z \end{array}\right]^T. \tag{5}$$

Equations (1) and (2) can be transformed to the following state equation.

$$\dot{\boldsymbol{x}} = \boldsymbol{A}_c\boldsymbol{x} + \boldsymbol{B}_c\boldsymbol{u} \tag{6}$$

where

$$\boldsymbol{A}_c = \left[\begin{array}{cc|cc} 0 & 1 & 0 & 0 \\ \omega^2 & 0 & 0 & 0 \\ \hline 0 & 0 & 0 & 1 \\ 0 & 0 & \omega^2 & 0 \end{array}\right], \ \boldsymbol{B}_c = \left[\begin{array}{c|c} 0 & 0 \\ -\omega^2 & 0 \\ \hline 0 & 0 \\ 0 & -\omega^2 \end{array}\right]. \tag{7}$$

Discretizing (6), we get

$$\boldsymbol{x}_{k+1} = \boldsymbol{A}\boldsymbol{x}_k + \boldsymbol{B}\boldsymbol{u}_k. \tag{8}$$

Note that in this system there is the constraint such that ZMP exists in the support polygon. In general, this ZMP constraint is represented by the following linear matrix inequality.

$$\boldsymbol{M}_k\boldsymbol{u}_k \leq \boldsymbol{v}_k. \tag{9}$$

Letting $\boldsymbol{m}_i^T$ and v_i be the i-th row vector of $\boldsymbol{M}_k$ and the i-th element of $\boldsymbol{v}_k$, respectively, the i-th edge of the support polygon is represented by the following equation.

$$\boldsymbol{m}_i^T\boldsymbol{u} = v_i. \tag{10}$$

III. Maximal Output Admissible Set for COG Regulator [18]

A. COG Regulation in the Upright Position

In order to stabilize the COG in the upright position, we consider a regulator that makes the state $\boldsymbol{x}$ converge to $\boldsymbol{x}_C = [\, x_C \; 0 \; y_C \; 0 \,]^T$. Let $\boldsymbol{p}_i = [\, x_i \; y_i \; z_i \,]^T (i = L, R)$ denote each foot position. For example, if we set x_C and y_C as follows:

$$x_C = \frac{x_L + x_R}{2}, \quad y_C = \frac{y_L + y_R}{2}, \tag{11}$$

the COG is controlled so that its projected point on the ground will be the center of both feet. Now, let us consider the following coordinate transformation.

$$\bar{\boldsymbol{x}} = \boldsymbol{x} - \boldsymbol{x}_C \tag{12}$$
$$\bar{\boldsymbol{u}} = \boldsymbol{u} - \boldsymbol{u}_C \tag{13}$$
$$\boldsymbol{u}_C := \left[\begin{array}{cc} x_C & y_C \end{array}\right]^T \tag{14}$$

Equations (8) and (9) are transformed to the following equations.

$$\bar{\boldsymbol{x}}_{k+1} = \boldsymbol{A}\bar{\boldsymbol{x}}_k + \boldsymbol{B}\bar{\boldsymbol{u}}_k \tag{15}$$
$$\boldsymbol{M}_k\bar{\boldsymbol{u}} \leq \bar{\boldsymbol{v}}_k \tag{16}$$
$$\bar{\boldsymbol{v}}_k := \boldsymbol{v}_k - \boldsymbol{M}_k\boldsymbol{u}_C \tag{17}$$

Equation (17) represents the coordinate transformation of the support polygon. In this section, we suppose the COG stabilization without stepping motion, in other words, $\boldsymbol{M}_k = \boldsymbol{M}$ (= const.) and $\boldsymbol{v}_k = \boldsymbol{v}$ (= const.) In order to control $\bar{\boldsymbol{x}}$ to the origin point $\boldsymbol{o}$, we apply the following state feedback.

$$\bar{\boldsymbol{u}}_k = -\boldsymbol{F}\bar{\boldsymbol{x}}_k \tag{18}$$

where $\boldsymbol{F}$ is a state feedback gain. Substituting (18) into (15), we get

$$\bar{\boldsymbol{x}}_{k+1} = \widetilde{\boldsymbol{A}}\bar{\boldsymbol{x}}_k \tag{19}$$
$$\widetilde{\boldsymbol{A}} := \boldsymbol{A} - \boldsymbol{B}\boldsymbol{F}. \tag{20}$$

We can design $\boldsymbol{F}$ by pole assignment or as the linear quadratic regulator (LQR) so that (19) becomes asymptotically stable.

B. Maximal Output Admisible Set [19][20]

If (19) is asymptotically stable, it is guaranteed that $\bar{\boldsymbol{x}}$ will converge to $\boldsymbol{o}$. However, it is not guaranteed that the constraint given by (16) will be satisfied with respect to time series of the input $\bar{\boldsymbol{u}}$. Whether the constraint will be satisfied depends on the initial value of $\bar{\boldsymbol{x}}$. If the constraint is not satisfied, the system becomes unstable because the necessary input cannot be generated. That means the ZMP reaches an edge of the support polygon and the contact between the foot sole and the ground becomes the edge contact. Therefore, it is important to check whether the constraint is satisfied during the control.

Based on this point of view, the Maximal Output Admissible (MOA) set [19][20] was proposed in the control engineering field as follows:

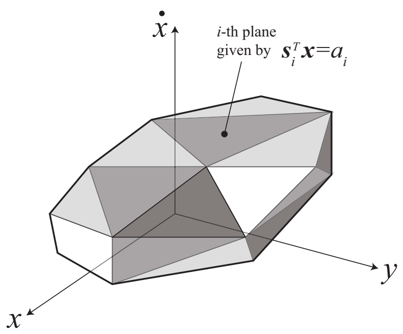

Fig. 2. MOA set projected onto x-y-$\dot{x}$ space

> Set of the initial value in which the constraint is satisfied with respect to series of the control input $\bar{\boldsymbol{u}}_k$ $(k = 0, \cdots, \infty)$.

Let O_∞ denote the MOA set on (19). If $\boldsymbol{x}_k \in O_\infty$, the constraint will be satisfied with respect to series of $\bar{\boldsymbol{u}}_k, \bar{\boldsymbol{u}}_{k+1}, \cdots$ while $\bar{\boldsymbol{x}}$ converges. O_∞ is defined as a convex polyhedron set in the state space, which is represented by the following form.

$$O_\infty = \{\boldsymbol{x} \in \mathbb{R}^4 | \boldsymbol{S}\bar{\boldsymbol{x}} \le \boldsymbol{a}\}. \tag{21}$$

In this paper, the state space is four-dimensional space, which consists of x, y, $\dot{x}$ and $\dot{y}$. Fig. 2 shows a schematic view of the MOA set projected onto the x-y-$\dot{x}$ space. Letting $\boldsymbol{s}_i^T$ and a_i be the i-th row vector of $\boldsymbol{S}$ and the i-th element of $\boldsymbol{a}$, respectively, the i-th plane of the convex polyhedron is represented by

$$\boldsymbol{s}_i^T \bar{\boldsymbol{x}} = a_i. \tag{22}$$

According to [19][20], we can compute $\boldsymbol{S}$ and $\boldsymbol{a}$ by iterations. Moreover, it is proved in [19][20] that this computation converges in finite number of iterations. $\boldsymbol{S}$ and $\boldsymbol{a}$ are calculated as follows:

$$\boldsymbol{S} = \begin{bmatrix} \boldsymbol{M} & \boldsymbol{O} & \cdots & \boldsymbol{O} \\ \boldsymbol{O} & \boldsymbol{M} & \cdots & \boldsymbol{O} \\ \vdots & \vdots & \ddots & \vdots \\ \boldsymbol{O} & \boldsymbol{O} & \cdots & \boldsymbol{M} \end{bmatrix} \begin{bmatrix} -\boldsymbol{F} \\ -\boldsymbol{F}\widetilde{\boldsymbol{A}} \\ \vdots \\ -\boldsymbol{F}\widetilde{\boldsymbol{A}}^n \end{bmatrix} \tag{23}$$

$$\boldsymbol{a} = \begin{bmatrix} \bar{\boldsymbol{v}}^T & \bar{\boldsymbol{v}}^T & \cdots & \bar{\boldsymbol{v}}^T \end{bmatrix}^T. \tag{24}$$

where n is the number of iterations, which depends on the feedback gain $\boldsymbol{F}$. The MOA set is based on a similar concept with the Model Predictive Control (MPC). Usually, finite number of steps is considered in MPC. On the other hand, we can consider infinite number of steps by using the MOA set.

IV. Maximal Output Admissible Set on Trajectory Tracking Controller

A. Tracking Control to COG Referential Trajectory

The previous section presented the MOA set a) on the COG regulator b) under the constant support polygon. In this section, we extend the MOA set to A) trajectory tracking controller B) under changing support polygon.

Suppose that a referential trajectory $\boldsymbol{\xi}_0, \cdots, \boldsymbol{\xi}_m$ is designed by a biped gait planning method, for example [4] or [5], so that the following requirements are satisfied.

1) The ZMP constraint given by (9) is satisfied.
2) At the end of the referential trajectory, the COG velocity is zero, namely, the robot stops.

In general, we can achieve the trajectory tracking control by the following controller.

$$\boldsymbol{u}_k = \boldsymbol{G}\boldsymbol{x}_k + \boldsymbol{H}\boldsymbol{\xi}_k \tag{25}$$

where $\boldsymbol{G}$ and $\boldsymbol{H}$ are controller gains. In most gait planning methods, we can generate not only the reference $\boldsymbol{x}_k$ but also corresponding ZMP, $\boldsymbol{\mu}_k$, which satisfies the following relationship.

$$\boldsymbol{\xi}_{k+1} = \boldsymbol{A}\boldsymbol{\xi}_k + \boldsymbol{B}\boldsymbol{\mu}_k \tag{26}$$

$\boldsymbol{\mu}_k$ is usually called *reference ZMP*. Using $\boldsymbol{\mu}_k$, we can also achieve the tracking control by the following controller.

$$\boldsymbol{u}_k = \boldsymbol{\mu}_k + \boldsymbol{F}(\boldsymbol{\xi}_k - \boldsymbol{x}_k) \tag{27}$$

This equation implies a 2-DOF controller in which the first and second terms in the right-hand side represent feedforward and feedback, respectively. In $k = 0, \cdots, m-1$, we apply the tracking controller given by (27). Then, after $k = m$, we apply the regulator given by (18) with $\boldsymbol{x}_C = \boldsymbol{\xi}_m$ in order to stop the robot.

B. Computational Procedure of Maximal Output Admissible Set for Trajectory Tracking Control

Let us consider the MOA set at $k = 0$. We can compute the MOA set by considering whether series of the input at $k = 0, \cdots, \infty$ satisfy the constraint. This computational procedure is divided into the following two phases.

i) Set of initial state, ${}^0O_{m-1}$, in which series of the input at $k = 0, \cdots, m-1$ generated by (27) satisfy the constraint.
ii) Set of initial state, ${}^{m-1}O_\infty$, in which series of the input at $k = m, \cdots, \infty$ generated by (18) satisfy the constraint.

First, we compute ${}^0O_{m-1}$. Substituting (27) into (8), we get

$$\boldsymbol{x}_{k+1} = \widetilde{\boldsymbol{A}}\boldsymbol{x}_k + \boldsymbol{B}(\boldsymbol{\mu}_k + \boldsymbol{F}\boldsymbol{\xi}_k) \tag{28}$$

From this recurrence formula, we can represent $\boldsymbol{x}_k$ by using the initial state $\boldsymbol{x}_0$ as follows:

$$\boldsymbol{x}_k = \widetilde{\boldsymbol{A}}^k \boldsymbol{x}_0 + \sum_{j=0}^{k-1} \widetilde{\boldsymbol{A}}^{k-j-1} \boldsymbol{B}(\boldsymbol{\mu}_j + \boldsymbol{F}\boldsymbol{\xi}_j) \tag{29}$$

Substituting (29) into (27), we get

$$\begin{aligned} \boldsymbol{u}_k = & -\boldsymbol{F}\widetilde{\boldsymbol{A}}^k \boldsymbol{x}_0 - \boldsymbol{F}\sum_{j=0}^{k-1} \widetilde{\boldsymbol{A}}^{k-j-1} \boldsymbol{B}(\boldsymbol{\mu}_j + \boldsymbol{F}\boldsymbol{\xi}_j) \\ & + (\boldsymbol{\mu}_k + \boldsymbol{F}\boldsymbol{\xi}_k) \end{aligned} \tag{30}$$

From (9) and (30), it is necessary that the initial state satisfies the following condition.

$${}^0\widehat{\boldsymbol{M}}_{m-1}\boldsymbol{\Phi}_{m-1}\boldsymbol{x}_0 \le {}^0\widehat{\boldsymbol{v}}_{m-1} - {}^0\widehat{\boldsymbol{M}}_{m-1}\boldsymbol{\Gamma}_{m-1}{}^0\boldsymbol{b}_{m-1} \tag{31}$$

where

$$
{}^{i}\widehat{\boldsymbol{M}}_{i+j} := \begin{bmatrix} \boldsymbol{M}_i & \boldsymbol{O} & \cdots & \boldsymbol{O} \\ \boldsymbol{O} & \boldsymbol{M}_{i+1} & \cdots & \boldsymbol{O} \\ \boldsymbol{O} & \boldsymbol{O} & \ddots & \boldsymbol{O} \\ \boldsymbol{O} & \boldsymbol{O} & \cdots & \boldsymbol{M}_{i+j} \end{bmatrix} \tag{32}
$$

$$
\boldsymbol{\Phi}_j := \begin{bmatrix} -\boldsymbol{F} \\ -\boldsymbol{F}\widetilde{\boldsymbol{A}} \\ \vdots \\ -\boldsymbol{F}\widetilde{\boldsymbol{A}}^{j} \end{bmatrix} \tag{33}
$$

$$
{}^{i}\widehat{\boldsymbol{v}}_{i+j} := \begin{bmatrix} \boldsymbol{v}_i^T & \boldsymbol{v}_{i+1}^T & \cdots & \boldsymbol{v}_{i+j}^T \end{bmatrix}^T \tag{34}
$$

$$
\boldsymbol{\Gamma}_j := \begin{bmatrix} \boldsymbol{I} & \boldsymbol{O} & \cdots & \boldsymbol{O} \\ -\boldsymbol{F}\boldsymbol{B} & \boldsymbol{I} & \cdots & \boldsymbol{O} \\ \vdots & \vdots & \ddots & \vdots \\ -\boldsymbol{F}\widetilde{\boldsymbol{A}}^{j-1}\boldsymbol{B} & -\boldsymbol{F}\widetilde{\boldsymbol{A}}^{j-2}\boldsymbol{B} & \cdots & \boldsymbol{I} \end{bmatrix} \tag{35}
$$

$$
{}^{i}\widehat{\boldsymbol{b}}_{i+j} := \begin{bmatrix} \boldsymbol{\mu}_i + \boldsymbol{F}\boldsymbol{\xi}_i \\ \boldsymbol{\mu}_{i+1} + \boldsymbol{F}\boldsymbol{\xi}_{i+1} \\ \vdots \\ \boldsymbol{\mu}_{i+j} + \boldsymbol{F}\boldsymbol{\xi}_{i+j} \end{bmatrix}. \tag{36}
$$

In (31), $i = 0$ and $j = m - 1$.

Next, we compute ${}^{m-1}O_\infty$. Using (29) and the coordinate transformation (12), we get

$$
\begin{aligned} \bar{\boldsymbol{x}}_m &= \boldsymbol{x}_m - \boldsymbol{\xi}_m \\ &= \widetilde{\boldsymbol{A}}^m \boldsymbol{x}_0 + \sum_{j=0}^{m-1} \widetilde{\boldsymbol{A}}^{k-j-1} \boldsymbol{B}(\boldsymbol{\mu}_j + \boldsymbol{F}\boldsymbol{\xi}_j) - \boldsymbol{\xi}_m. \end{aligned} \tag{37}
$$

Now, we consider $\bar{\boldsymbol{x}}_m$ as the initial state. From the MOA set on the regulator presented in the previous section, we can formulate the condition that series of the input $\boldsymbol{u}_m, \cdots, \boldsymbol{u}_\infty$ should satisfy as follows:

$$
\boldsymbol{S}\bar{\boldsymbol{x}}_m \leq \boldsymbol{a}. \tag{38}
$$

Substituting (37) into (38), we get

$$
\boldsymbol{S}\widetilde{\boldsymbol{A}}^m \boldsymbol{x}_0 \leq \boldsymbol{a} + \boldsymbol{S}\left\{ \boldsymbol{\xi}_m - \sum_{j=0}^{m-1} \widetilde{\boldsymbol{A}}^{k-j-1} \boldsymbol{B}(\boldsymbol{\mu}_j + \boldsymbol{F}\boldsymbol{\xi}_j) \right\}. \tag{39}
$$

Summarizing the above discussion, ${}^0O_{m-1}$ and ${}^{m-1}O_\infty$ are represented by (31) and (39), respectively. Therefore, the MOA set at $k = 0$ is computed as follows:

$$
{}^0O_\infty = {}^0O_{m-1} \cap {}^{m-1}O_\infty. \tag{40}
$$

This type of the MOA set results in time-variant set, like ${}^0O_\infty, {}^1O_\infty, \cdots, {}^{m-1}O_\infty$. In general, ${}^kO_\infty$ is represented by

$$
{}^kO_\infty = {}^kO_{m-1} \cap {}^{m-1}O_\infty, \tag{41}
$$

and we can compute ${}^kO_{m-1}$ by replacing 0 with k in (41).

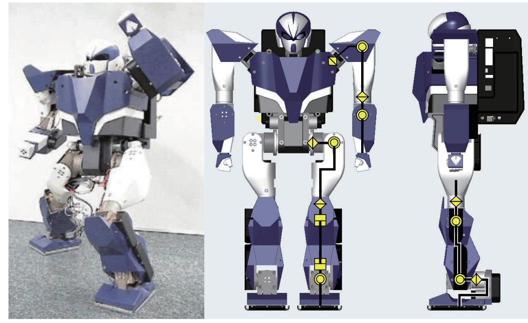

Main specification

Height : 54[mm]

Weight : 8.0[kg]

Number of joints : 20 (4 at each arms, 6 at each legs)

Fig. 3. External view of UT-μ2

C. Example of Computation

As an example, we computed the MOA set for tracking control of a walking motion. We generated a walking motion for UT-μ2, a small-size humanoid robot as shown in Fig. 3, by using a biped gait planning method proposed in [5]. Fig. 4 shows the walking motion. The motion consists of total four steps, in which each step takes 0.5[s] and the stride is 0.1[m]. The upper of Fig. 4 shows snapshots of the referential COG (blue point), ZMP (red point), each foot position (black points) and corresponding support polygon (green region).

Fig. 5 shows the result of the MOA set for the walking motion. The feedback gain was designed as the LQR. Fig. 5(a) shows a projection of the MOA set on the x-$\dot{x}$ plane. We observe that the MOA set shifts in $+x$ direction as the robot walks forward. Moreover, Fig. 5(b) shows a projection of the MOA set on the y-$\dot{y}$ plane. We observe that the MOA set shifts in y direction as the robot rolls to left and right.

In Fig. 5(b), the MOA set at $t = 2.0$s is larger than other four. It is considered that this is because the MOA sets between t =0s and 5s are given by ${}^kO_{m-1} \cap {}^mO_\infty$ whereas the MOA set at t =2.0s is given by only ${}^mO_\infty$. Therefore, the MOA set at t <2.0s becomes smaller by ${}^kO_{m-1}$. On the other hand, this consideration does not apply to Fig. 5(a). This is because the larger support polygon results in the larger MOA set, and the support polygon at t =0.5s, 1.0s, 1.5s in Fig. 5(a) is larger than t =0s, 2.0s.

V. Application to Falling Avoidance Control

We extend the MOA set framework to falling avoidance control. Suppose that at the initial state the robot stands with both feet together, and the COG is controlled so that its projected point on the ground converges to the center of the support polygon. The blue region in Fig. 6 indicates the MOA set for the COG regulator, ${}^rO_\infty$. On the other hand, the green region indicates the MOA set for a tracking controller to a forward stepping motion, ${}^tO_\infty$. We observe that ${}^tO_\infty$ shifts in $+x$ or $+\dot{x}$ direction compared to ${}^rO_\infty$. When the robot is pushed from the back, the COG state exists from ${}^rO_\infty$ to ${}^tO_\infty$. In this case, it is possible to avoid falling by switching controllers from the COG regulator to the tracking controller.

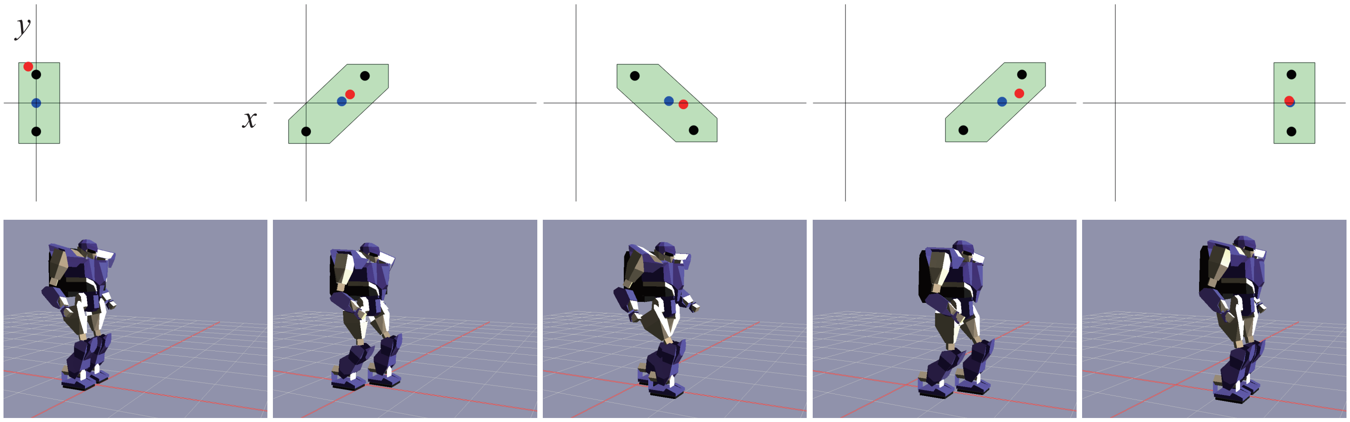

Fig. 4. Referential trajectory of a walking motion. The upper shows snapshots of the referential COG (blue point), ZMP (red point), each foot position (black points) and corresponding support polygon (green region).

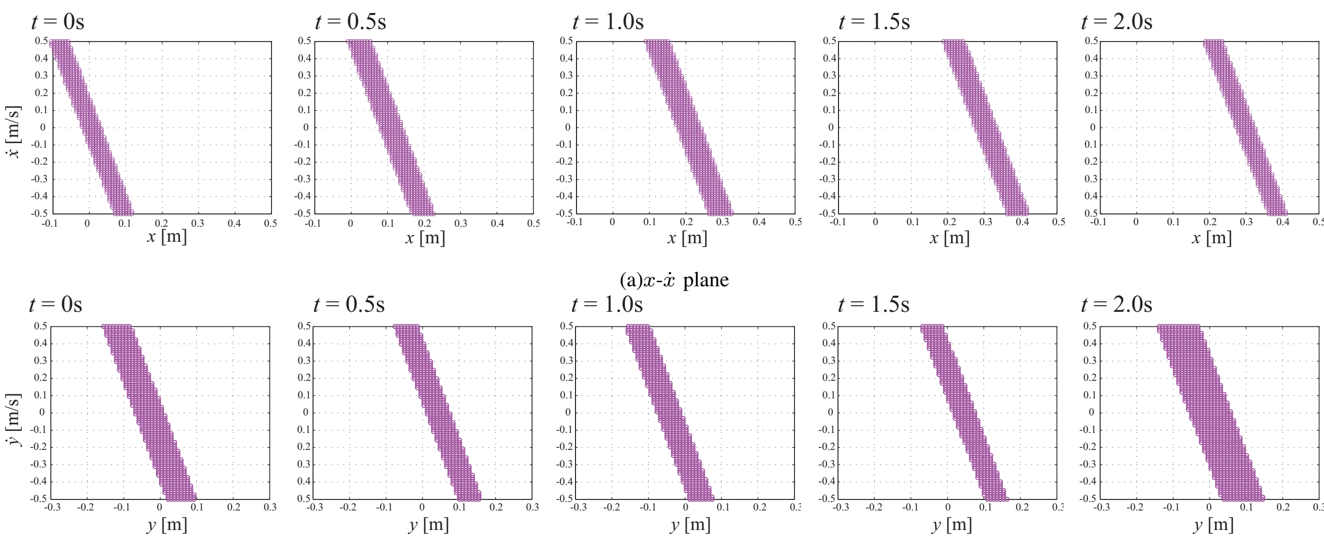

(a)x-$\dot{x}$ plane

(b)y-$\dot{y}$ plane

Fig. 5. Maximal output admissible set in the trajectory tracking control

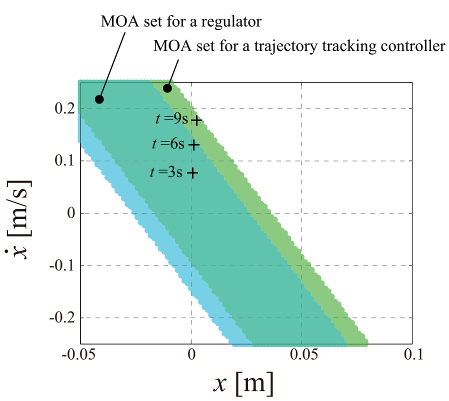

Fig. 6. Maximal output admissible sets of a regulator in the upright position (blue region) and tracking controller to a stepping motion (green region)

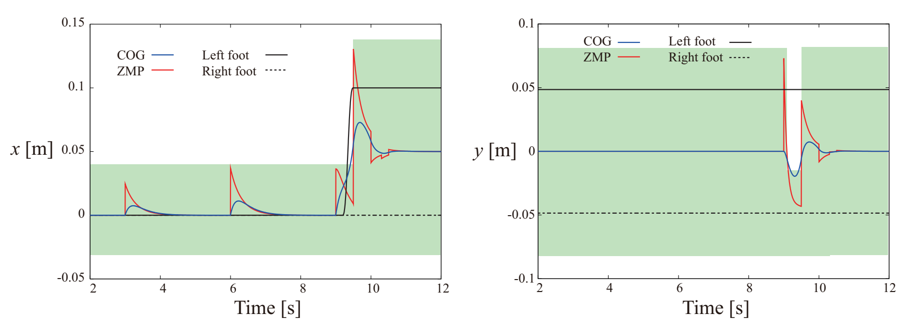

Fig. 7. Simulation results of COG, ZMP and both feet position in the falling avoidance control

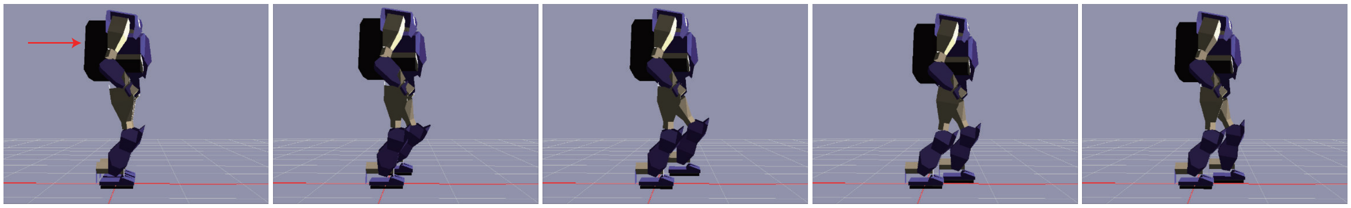

Fig. 8. Falling avoidance control by switching the regulator and the trajectory tracking controller based on the MOA set

We simulated the proposed falling avoidance control. In the simulation, we added disturbances three times (at t =3s, 6s, 9s) in $+x$ direction. Those disturbances became larger in order of t =3s, 6s, 9s. Due to the disturbances, the COG state jumped from the origin point, as indicated by $+$ in Fig. 6. It is observed that at t = 9s the COG state exceeded ${}^{r}O_{\infty}$. In this case, we can prevent the robot from falling by using the trajectory tracking controller. Fig. 7 shows trajectories of the COG (blue), ZMP (red), each foot position (black lines) and the support polygon (green region). After t =9s, it is observed that the controller is switched to the trajectory tracking controller and the robot steps forward. Fig. 8 shows the resultant falling avoidance motion. Although this simulation not is based on full-body dynamic model but the COG-ZMP inverted pendulum model, we can verify that the MOA set is applicable to the falling avoidance control with controller switching.

VI. Conclusion

This paper presented the computational procedure of the MOA set for a trajectory tracking control of biped robots. It was verified that we can compute the MOA set even when the trajectory and constraint are time-variant. Moreover, this extension made it possible to switch the COG regulator and tracking control based on the MOA set. We applied this framework to a falling avoidance control and verified its validity with simulations.

In future works, we will extend the MOA set framework to limit cycle type controller and tracking control to running and hopping. The extension to the limit cycle type controller makes it possible to switch the upright balancing and periodic stepping or walking motion. The extension to the hopping motion makes it possible to avoid falling by hopping.

References

[1] M. Vukobratović and D. Juricić, "Contribution to the Synthesis of Biped Gait," *IEEE Transactions on Biomedical Engineering*, vol. 16, no. 1, pp. 1–6, 1969.

[2] A. Takanishi *et al.*, "Realization of Dynamic Biped Walking Stabilized by Trunk Motion on a Sagittally Uneven Surface," in *Proc. of IEEE International Workshop on Intelligent Robots and Systems*, 1990, pp. 323–330.

[3] K. Nishiwaki *et al.*, "Generation of Reactive Stepping Motion for a Humanoid by Dynamically Stable Mixture of Pre-designed Motions," in *Proc. of IEEE International Conference on Systems, Man, and Cybernetics*, 1999, pp. 902–907.

[4] K. Harada *et al.*, "An Analytical Method on Real-time Gait Planning for a Humanoid Robot," in *Proc. of the 4th IEEE/RAS International Conference on Humanoid Robots*, 2004, pp. 640–655.

[5] T. Sugihara and Y. Nakamura, "Boundary Condition Relaxation Method for Stepwise Pedipulation Planning of Biped Robots," *IEEE Transaction on Robotics*, vol. 25, no. 3, pp. 658–669, 2009.

[6] L. Kovar *et al.*, "Motion graphs," *ACM Transactions on Graphics*, vol. 21, no. 3, pp. 1–10, July 2002.

[7] K. Yamane and Y. Nakamura, "Dynamics Filter-Concept and Implementation of Online Motion Generator for Human Figures," *IEEE Transactions on Robotics and Automation*, vol. 19, no. 3, pp. 421–432, June 2003.

[8] S. Kagami *et al.*, "Autobalancer: An online dynamic balance compensation scheme for humanoid robots," in *Proc. Int. Workshop Alg. Found. Robot.(WAFR)*, 2000.

[9] S. Kajita *et al.*, "Balancing a Humanoid Robot Using Backdrive Concerned Torque Control and Direct Angular Momentum Feedback," in *Proc. of IEEE International Conference on Robotics and Automation*, 2001, pp. 3376–3382.

[10] M. Abdallah and A. Goswami, "A Biomechanically Motivated Two-Phase Strategy for Biped Upright Balance Control," in *Proc. of IEEE International Conference on Robotics and Automation*, 2005, pp. 1996–2001.

[11] C. G. Atkeson and B. Stephens, "Multiple Balance Strategies from One Optimization Criterion," in *Proc. of IEEE-RAS International Conference on Humanoid Robots*, 2007, pp. 57–64.

[12] R. Katoh and M. Mori, "Control Method of Biped Locomotion Giving Asymptotic Stability of Trajectory," *Automatica*, vol. 20, no. 4, pp. 405–414, 1984.

[13] J. Morimoto *et al.*, "A Biologically Inspired Biped Locomotion Strategy for Humanoid Robots: Modulation of Sinusoidal Patterns by a Coupled Oscillator Model," *IEEE Transactions on Robotics*, vol. 24, no. 1, pp. 185–191, 2008.

[14] B. Stephens and C. Atkeson, "Modeling and Control of Periodic Humanoid Balance using the Linear Biped Model," in *Proc. of IEEE-RAS International Conference on Humanoid Robots*, 2009, pp. 379–384.

[15] T. Sugihara, "Biped Control to Follow Arbitrary Referential Longitudinal Velocity based on Dynamics Morphing," in *Proc. of the 2012 IEEE/RSJ International Conference on Intelligent Robots and Systems*, Oct. 2012, pp. 1892–1897.

[16] U. Muico *et al.*, "Contact-aware Nonlinear Control of Dynamic Characters," *ACM Transactions on Graphics*, vol. 28, no. 3, 2009.

[17] A. Herdt *et al.*, "Online Walking Motion Generation with Automatic Foot Step Placement," *Advanced Robotics*, vol. 24, pp. 719–737, 2010.

[18] K. Yamamoto and Y. Nakamura, "Switching Feedback Controllers Based on the Maximal CPI Sets for Stabilization of Humanoid Robots," in *Proc. of the 9th IEEE-RAS International Conference on Humanoid Robots*, 2009, pp. 549–554.

[19] E. Gilbert and K. Tan, "Linear Systems with State and Control Constraints: The Theory and Application of Maximal Output Admissible Sets," *IEEE Transactions on Automatic Control*, vol. 36, no. 9, pp. 1008–1020, 1991.

[20] K. Hirata and M. Fujita, "Analysis of Conditions for Non-Violation of Constraints on Linear Dicrete-time Systems with Exogenous Inputs," in *Proc. of the 36th IEEE Conference on Decision and Control*, 1997, pp. 1477–1478.

[21] M. Vukobratović and J. Stepanenko, "On the Stability of Anthropomorphic Systems," *Mathematical Biosciences*, vol. 15, pp. 1–37, 1972.

[22] K. Kogiso and K. Hirata, "Reference Governor for Constrained Systems with Time-Varying References," *Robotics and Autonomous Systems*, vol. 57, no. 3, pp. 289–295, 2009.